ELSEVIER

International Journal of Solids and Structures 41 (2004) 5265–5284

INTERNATIONAL JOURNAL OF SOLIDS and STRUCTURES

www.elsevier.com/locate/ijsolstr

The shock pattern for axially symmetric shear wave propagation in a hyperelastic incompressible solid

D.W. Barclay *

Department of Mathematics and Statistics, University of New Brunswick, Post Office Box 4400, Fredericton, Canada E3B 5A3

Received 25 July 2003; received in revised form 6 March 2004
Available online 12 May 2004

Abstract

Here we consider axially symmetric shear waves propagating from a cylindrical cavity in an incompressible hyperelastic solid, whose strain energy function is expressible as a truncated power series in terms of the basic strain invariants. The solid is assumed to be unbounded. A continuous pulse is initiated at the boundary of the cavity and can break in finite time. We determine what shock waves can subsequently occur using an approximate solution obtained by Whitham's nonlinearization technique. We find that under mild restrictions on the material parameters, a shock wave develops near the front or back of the pulse, and propagates indefinitely. In addition, a *transient shock* can occur and exist for a finite length of time. The set of shock paths will be referred to as the *shock pattern*. We show how the material parameters influence the shock pattern. As well, the analysis presented here provides accurate estimates of the breaking distance and time, and the location of the shock path, for any shock waves that occur. Results of the analysis are illustrated with numerical solutions obtained using a relaxation scheme for systems of conservation laws.

Keywords: Shock wave; Elastic solid

1. Introduction

Axially symmetric shear wave propagation from a cylindrical cavity in an unbounded hyperelastic material is considered. A wave is initiated at the boundary of the cavity by a continuous pulse of finite duration time. A continuous wave propagates into the material and can break in finite time. We determine what possible shock waves can occur and how the material parameters influence their development. The set of shock paths together with any wavefronts will be referred to as the *shock pattern*.

The propagation of nonlinear axially symmetric shear waves from a cylindrical cavity was first studied by Haddow et al. (1987a,b) and Tait et al. (1989). These papers were primarily concerned with obtaining numerical solutions. The problem of a shock front propagating from a cylindrical cavity was considered by

* Tel.: +1-506-453-4768; fax: +1-506-453-4705.
E-mail address: dave@math.unb.ca (D.W. Barclay).

0020-7683/$ - see front matter © 2004 Elsevier Ltd. All rights reserved.
doi:10.1016/j.ijsolstr.2004.04.006

Barclay (1999), where formulas for the shock speed and strength were found. Transverse cylindrical waves had also been considered by Fu and Scott (1991), where a modulated simple wave solution was obtained and used to fit a shock wave initiated at the boundary of a cylindrical cavity. None of the above papers analysed the various shock waves that can occur after a continuous wave breaks.

We consider wave propagation into a medium that is assumed to be an incompressible hyperelastic solid, whose strain energy function is expressible as a power series Ogden (1984),

$$W(I_1, I_2) = \sum_{i,j=0}^{\infty} C_{ij}(I_1 - 3)^i (I_2 - 3)^j. \tag{1.1}$$

The quantities I_1 and I_2 are the first and second strain invariants and C_{ij} are constants with $C_{00} = 0$. Several special cases of (1.1), which involve only the first few terms, have appeared in the literature. For example, the special case

$$W = C_{10}(I_1 - 3) + C_{01}(I_2 - 3) \tag{1.2}$$

is the strain energy function for the Mooney–Rivlin material, while $C_{01} = 0$ in (1.2) results in the Neo-Hookean strain energy function. In the present work, we employ the strain energy function obtained when (1.1) is truncated so that $\max(i + j) = N + 1$. For this case, the strain energy function has the form

$$W = \sum_{k=0}^{N} \sum_{i=0}^{k+1} C_{i,k-i+1}(I_1 - 3)^i (I_2 - 3)^{k-i+1}. \tag{1.3}$$

Numerical values of the material constants C_{ij} in (1.3) have been found for various materials by Alexander (1968), Tschoegl (1971), James et al. (1975) and Haines and Wilson (1979), using least squares fitting of experimental data.

In this paper, we determine the shock pattern for axial shear waves. The analysis is essentially the same for torsional shear waves, while the problem of combined axial and torsional shear wave propagation is more difficult and requires further investigation.

In Barclay (2004), we obtained and used an approximate solution to estimate the breaking time of a nonlinear axial shear wave. The approximate solution was constructed using the nonlinearization technique described in Chapter 9 of Whitham (1974). Here, we use this approximate solution to determine the shock pattern. Our analysis reveals all the possible shocks that can occur. In addition to shocks which propagate indefinitely, we discover that another shock can develop and exist for a finite length of time. We call such a shock, a *transient shock*. A transient shock path has finite length. A shock with this property had not been described in the earlier mentioned papers on axially symmetric shear wave propagation. Our results provide conditions on the material parameters for which a transient shock will or will not exist.

The shock patterns described here are for a disturbance generated at the boundary of the cavity by a continuously rising boundary value of finite duration time. In order to carry out the analysis, it is necessary to assume that the derivative of a certain function h related to the boundary value has a particular behavior. This assumption does not appear to be a severe restriction. We elaborate on this point in Section 3. As well, for a continuously rising boundary value, all field variables are continuous across the leading wavefront, and a wavefront expansion can be calculated. As shown by Tait et al. (1989), an axially symmetric shear wave never breaks at the wavefront. Consequently, a wavefront analysis provides no information concerning the breaking of a wave.

Finally, we illustrate our shock results by numerically solving the system of partial differential equations governing axially symmetric shear wave propagation. We use the nonoscillatory scheme for systems of conservation laws proposed by Jin and Xin (1995).

2. Formulation and approximate solution

In this section, we list the equations governing combined axial and torsional shear wave propagation. We then summarize the nonlinarized solution for axial shear wave propagation that is used to carry out the shock pattern analysis in the next section.

Time dependent axially symmetric shear of an incompressible solid is defined by the deformation field

$$r = R, \quad \theta = \Theta + \beta(R,t), \quad z = Z + w(R,t), \tag{2.1}$$

where (R,Θ,Z) and (r,θ,z) are cylindrical coordinates of a particle in the reference and spatial configurations respectively, and t is time. The governing equations for axially symmetric shear are obtained from the constitutive equation for an incompressible hyperelastic solid, together with the equations of motion. We list the relevent equations used here. For a more detailed description of the formulation of the equations, see Haddow et al. (1987a).

For the deformation field defined by (2.1), the principal invariants of the left Cauchy–Green tensor are

$$I_1 = I_2 = 3 + \Delta^2, \quad I_3 = 1, \tag{2.2}$$

where

$$\Delta = \sqrt{\epsilon^2 + (r\delta)^2} \tag{2.3}$$

and

$$\epsilon = \frac{\partial w}{\partial r}, \quad \delta = \frac{\partial \beta}{\partial r}. \tag{2.4}$$

The quantities Δ, ϵ and δ are dimensionless variables. Since $I_3 = 1$, the deformation field is incompressible. Using the constitutive equation and the strain energy function (1.3), the shear components $\tau_{r\theta}$ and τ_{rz} of the Cauchy stress tensor in cylindrical coordinates are given by

$$\tau_{r\theta} = \mu V(\Delta) r\delta, \quad \tau_{rz} = \mu V(\Delta)\epsilon, \tag{2.5}$$

where

$$V(\Delta) = 1 + 2\sum_{k=1}^{N} \gamma_k \Delta^{2k}, \tag{2.6}$$

$$\gamma_k = \frac{k+1}{\mu} \sum_{i=0}^{k+1} C_{i,k+1-i} \tag{2.7}$$

and

$$\mu = 2(C_{10} + C_{01}) \tag{2.8}$$

is the modulus of rigidity for infinitesimal deformation. The components of torsional and axial shear stress in (2.5) are physical components and similar expressions can be obtained for the remaining four components of stress. We note that for the material constants C_{ij} found by Alexander (1968), Tschoegl (1971), James et al. (1975) and Haines and Wilson (1979), the corresponding values of the nondimensional quantities $\gamma_k, k = 1, N$ all satisfy $|\gamma_k| \ll 1$ and for many materials have differing signs. For convenience, we let

$$\boldsymbol{\gamma} = (\gamma_1, \gamma_2, \ldots, \gamma_N)$$

denote the vector of material parameters and define

$$\|\boldsymbol{\gamma}\| = \sum_{k=1}^{N} |\gamma_k|.$$

For the Mooney–Rivlin or Neo-Hookean material $\gamma = \mathbf{0}$, and the relations in (2.5) are linear.

Employing the equations of motion and introducing the variables

$$\omega = \frac{\partial \beta}{\partial t}, \quad v = \frac{\partial w}{\partial t}, \tag{2.9}$$

we obtain the system of equations consisting of (2.5) and

$$\frac{\partial \tau_{r\theta}}{\partial r} + \frac{2\tau_{r\theta}}{r} = \rho r \frac{\partial \omega}{\partial t}, \tag{2.10}$$

$$\frac{\partial \tau_{rz}}{\partial r} + \frac{\tau_{rz}}{r} = \rho \frac{\partial v}{\partial t}, \tag{2.11}$$

$$\frac{\partial \delta}{\partial t} = \frac{\partial \omega}{\partial r}, \quad \frac{\partial \epsilon}{\partial t} = \frac{\partial v}{\partial r}, \tag{2.12}$$

where ρ is the constant material density. When $\gamma = \mathbf{0}$, the system uncouples into two linear systems, one governing the propagation of axial shear waves and the other governing the propagation of torsional shear waves, both with wave speed

$$c = \sqrt{\frac{\mu}{\rho}}.$$

We consider the propagation of waves from a cylindrical cavity, of radius a, in an unbounded medium which is initially unstressed and at rest. The axis of the cavity coincides with the z-axis of the cylindrical coordinate system. A disturbance is initiated by spatially uniform shearing tractions applied to the surface of the cavity. Hence our system (2.5), (2.10)–(2.12) is subject to quiescent initial conditions and the boundary conditions

$$\tau_{rz}(a,t) = f(t)H(t), \quad \tau_{r\theta}(a,t) = g(t)H(t), \tag{2.13}$$

where $f(t)$, $g(t)$ are given functions and $H(t)$ is the Heaviside unit function. Later, we shall consider in detail axial shear waves generated by the boundary value

$$f(t) = \sigma_0 \sin\frac{\pi t}{t_*}[H(t) - H(t - t_*)], \tag{2.14}$$

which represents a pulse of duration t_* and maximum of σ_0.

We now introduce nondimensional variables defined by

$$(\hat{\tau}_{r\theta}, \hat{\tau}_{rz}, \hat{\sigma}_0) = (\tau_{r\theta}, \tau_{rz}, \sigma_0)/\mu, \quad (\hat{w}, \hat{r}) = (w, r)/a, \quad (\hat{t}, \hat{t}_*) = (t, t_*)c/a,$$

$$\hat{v} = v/c, \quad \hat{\omega} = a\omega/c, \quad \hat{\epsilon} = \epsilon, \quad \hat{\delta} = a\delta, \quad \hat{c} = 1, \quad \hat{a} = 1.$$

Henceforth, we will use nondimensional variables, but for convenience omit the carets. The nondimensional form of the Eqs. (2.5), (2.10)–(2.12) is then

$$\tau_{r\theta} = V(\Delta) r\delta, \quad \tau_{rz} = V(\Delta)\epsilon, \tag{2.15}$$

$$\frac{\partial \tau_{rz}}{\partial r} + \frac{\tau_{rz}}{r} = \frac{\partial v}{\partial t}, \tag{2.16}$$

$$\frac{\partial \tau_{r\theta}}{\partial r} + \frac{2\tau_{r\theta}}{r} = r\frac{\partial \omega}{\partial t}, \tag{2.17}$$

$$\frac{\partial \epsilon}{\partial t} = \frac{\partial v}{\partial r}, \quad \frac{\partial \delta}{\partial t} = \frac{\partial \omega}{\partial r}. \tag{2.18}$$

If we eliminate the shear stresses $\tau_{r\theta}$ and τ_{rz} from the above equations, we obtain a hypberbolic system of partial differential equations in terms of the vector

$$\mathbf{u} = \begin{pmatrix} u_1 \\ u_2 \\ \epsilon \\ \delta \end{pmatrix},$$

where

$$u_1 = rv, \quad u_2 = r^3\omega.$$

This system can be written in conservation form as

$$\mathbf{u}_t + \mathbf{f}(\mathbf{u}, r)_r = \mathbf{0}, \quad r > 1, \quad t > 0, \tag{2.19}$$

where the inhomogeneous flux function is given by

$$\mathbf{f} = \begin{pmatrix} -rV(\Delta)\epsilon \\ -r^3V(\Delta)\delta \\ -u_1/r \\ -u_2/r^3 \end{pmatrix}. \tag{2.20}$$

For axial shear waves propagating alone, $\beta = 0$ in (2.1). For this case, the analysis leads to a conservation law (2.19) with

$$\mathbf{u} = \begin{pmatrix} u_1 \\ \epsilon \end{pmatrix}, \quad \mathbf{f} = \begin{pmatrix} -rV(\epsilon)\epsilon \\ -u_1/r \end{pmatrix}. \tag{2.21}$$

For torsional shear waves propagating alone $w = 0$, and the conservation law for torsional wave propagation is expressed in terms of

$$\mathbf{u} = \begin{pmatrix} u_2 \\ \delta \end{pmatrix}, \quad \mathbf{f} = \begin{pmatrix} -r^3V(r\delta)\delta \\ -u_2/r^3 \end{pmatrix}. \tag{2.22}$$

An approximate solution to (2.19) with (2.21) for axial shear waves was obtained by Barclay (2004) using Whitham's nonlinearization technique. A similar solution can be obtained for torsional shear waves propagating alone, but a solution cannot be constructed in an analogous way for combined axial and torsional shear wave propagation. This problem is complicated by the fact that the governing system (2.19) with (2.20) has two families of outgoing characteristics, and the nonlinearization technique does not apply. The solution for axial shear is described next.

If $\boldsymbol{\gamma} = \mathbf{0}$, then the system (2.19) is linear and can be solved by the Laplace transform

$$\bar{f}(p) = \mathscr{L}\{f(t)\} = \int_0^\infty \mathrm{e}^{-pt} f(t)\,\mathrm{d}t.$$

We construct the function

$$\Phi(r, \alpha) = \frac{1}{r}\int_0^\alpha \frac{(\alpha + r - \eta)F(\eta)}{\sqrt{(\alpha - \eta)(\alpha - \eta + 2r)}}\,\mathrm{d}\eta \tag{2.23}$$

from the linear solution, where

$$F(t) = \mathscr{L}^{-1}\left\{ \frac{\bar{\phi}(p)\mathrm{e}^{-p}}{K_1(p)} \right\}, \tag{2.24}$$

$$\phi(t) = \epsilon(1,t) \tag{2.25}$$

and $K_n(x)$ is the modified Bessel function of the second kind. Then the approximate solution to the nonlinear problem is

$$\epsilon \approx \Phi(r,\alpha) \tag{2.26}$$

on

$$t = r - 1 + \alpha - \sum_{k=1}^{N}(2k+1)\gamma_k \int_1^r \Phi^{2k}(r,\alpha)\,\mathrm{d}r, \tag{2.27}$$

where the integration is carried out holding α constant. Eq. (2.27) defines $\alpha(r,t)$ implicitly and the combined equations (2.26) and (2.27) provide a "nonlinearized" solution to the axial shear problem valid behind the leading wavefront. The family of outgoing characteristics are given by $\alpha(r,t) = \text{const}$. It was shown by Barclay (2004) that the above approximate solution is the leading term in a uniform expansion valid for small values of the parameter $\|\boldsymbol{\gamma}\|$. Regarding $\|\boldsymbol{\gamma}\|$ as a small parameter is a reasonable assumption, since as we noted earlier, $|\gamma_k| \ll 1$ for many real materials.

In the next section, we use the solution (2.26) and (2.27) to analyse shock development of an axial shear wave. This solution can be written as

$$\Phi(r,\alpha) = \frac{1}{\sqrt{2r}} \int_0^\alpha \frac{F(\eta)}{\sqrt{\alpha-\eta}} \frac{1+\frac{\alpha-\eta}{r}}{\sqrt{1+\frac{\alpha-\eta}{2r}}}\,\mathrm{d}\eta \tag{2.28}$$

and then expanded, using the binomial theorem, as the series

$$\Phi(r,\alpha) = \sum_{k=0}^{\infty} \frac{(-1)^{k-1}(2k+1)!}{2^{2k}(k!)^2(2k-1)} \left(\frac{1}{2r}\right)^{k+\frac{1}{2}} \int_0^\alpha (\alpha-\eta)^{k-\frac{1}{2}} F(\eta)\,\mathrm{d}\eta, \tag{2.29}$$

convergent for $0 \leqslant \frac{\alpha}{2r} < 1$. In order to carry out our shock analysis, we make the further assumption that $\frac{\alpha}{r} \ll 1$. We then simplify the solution using the leading term from (2.29), i.e.

$$\Phi(r,\alpha) = \sqrt{\frac{\pi}{2r}} G(\alpha) + \mathrm{O}\left[\left(\frac{\alpha}{r}\right)^{\frac{3}{2}}\right], \tag{2.30}$$

where

$$G(t) = \frac{1}{\sqrt{\pi}} \int_0^t \frac{F(\eta)}{\sqrt{t-\eta}}\,\mathrm{d}\eta = \mathscr{L}^{-1}\left\{ \frac{\bar{\phi}(p)\mathrm{e}^{-p}}{\sqrt{p}K_1(p)} \right\}, \quad t \geqslant 0. \tag{2.31}$$

Our approximate solution now becomes

$$\epsilon \approx \sqrt{\frac{\pi}{2r}} G(\alpha) \tag{2.32}$$

on

$$t = r - 1 + \alpha - \sum_{k=1}^{N}(2k+1)\gamma_k h^k(\alpha) S_k(r), \quad \alpha \geqslant 0, \tag{2.33}$$

where

$$h(\alpha) = \frac{\pi}{2} G^2(\alpha) \tag{2.34}$$

and

$$S_k(r) = \int_1^r \frac{\mathrm{d}r}{r^k} = \begin{cases} \ln r, & k = 1, \\ \dfrac{1 - r^{1-k}}{k-1}, & k \geqslant 2. \end{cases} \tag{2.35}$$

Eq. (2.33) is an approximate formula for the family of outgoing characteristics to our nonlinear axial shear wave problem. The parameter α labels the characteristics and small values of α correspond to characteristics near the leading wavefront. The pair of Eqs. (2.32) and (2.33) provide an approximate solution to the problem valid for small values of the parameter $\|\gamma\|$ and for $\frac{\alpha}{r} \ll 1$, i.e. near the leading wavefront or at large distances. The solution reveals that geometric attenuation is of order $r^{-\frac{1}{2}}$.

In view of (2.31), the solution does not involve the surface traction $f(t)$ directly but is expressed in terms of $\phi(t)$. Since $\phi(t)$ is defined by (2.25), it must be found from $f(t)$ through the constitutive equation, i.e.

$$f = U(\phi) \equiv \phi + 2\sum_{k=1}^{N} \gamma_k \phi^{2k+1}. \tag{2.36}$$

So for a given surface traction $f(t)$, the existence of $\phi(t)$ implies certain restrictions on the material parameters. The following result will be useful in later work.

Theorem 1. *Suppose that $f(t)$ is continuous on $t \geqslant 0$ and $f(0) = 0$.*

(i) *Eq.* (2.36) *defines a continuous function $\phi(t)$ on $0 \leqslant t \leqslant T$ for some $T > 0$ and $\phi(0) = 0$.*

(ii) *If $U'(\phi) \geqslant 0$ for all ϕ, then $T = \infty$ in* (i).

(iii) *If $0 \leqslant f(t) \leqslant \sigma_0 = f(t_0)$ for $t \geqslant 0$, and $U'(\phi) \geqslant 0$ for $0 \leqslant \phi \leqslant \phi_0$, where $\sigma_0 \leqslant U(\phi_0)$, then $T = \infty$ in* (i). *Also*

$$0 \leqslant \phi(t) \leqslant \epsilon_0 = \phi(t_0),$$

where ϵ_0 is the smallest solution to

$$\sigma_0 = U(\epsilon_0). \tag{2.37}$$

3. The shock pattern

Shear waves are generated at the boundary of an unstressed material by surface tractions (2.13). If $f(t)$ and $g(t)$ are continuous and

$$f(0) = g(0) = 0,$$

then a continuous wave propagates into the material. The wave can break in finite time and a shock will develop. We investigate what possible shock paths can occur. We carry out the details of our calculations for axial shear wave propagation. The results for torsional shear waves will be similar, while the case of combined axial and torsional shear waves requires further study.

To determine the possible shock paths for axial shear waves, we construct the envelope for the family of characteristics (2.33). The envelope bounds regions in which the solution is multivalued and within which a shock path must be fitted. Differentiating (2.33) with respect to α gives

$$L(r, \alpha) = \frac{1}{h'(\alpha)}, \tag{3.1}$$

where

$$L(r,\alpha)=\sum_{k=1}^{N}k(2k+1)\gamma_k h^{k-1}(\alpha)S_k(r). \tag{3.2}$$

We denote any real solution of (3.1) for $r>1$ by

$$r=E(\alpha) \tag{3.3}$$

and let

$$t=T(\alpha) \tag{3.4}$$

be the function obtained on using (3.3) in (2.33). The functions $E(\alpha)$ and $T(\alpha)$ have the same domain, which is a subset of $\alpha>0$, and (3.3), (3.4) are approximate parametric equations of the envelope. The approximations are valid provided $\|\boldsymbol{\gamma}\|\ll 1$ and $\frac{\alpha}{r}\ll 1$. We note that if $N=1$, then E and T can be found explicitly and are

$$E(\alpha)=\exp\{\left[3\gamma_1 h'(\alpha)\right]^{-1}\},\quad T(\alpha)=E(\alpha)-1+\alpha-\frac{h(\alpha)}{h'(\alpha)}. \tag{3.5}$$

The envelope constructed from Eq. (3.1) can be used to determine the shock pattern for axial shear waves generated by any surface traction $f(t)$, provided we know certain analytic properties of $h(\alpha)$ and its derivative $h'(\alpha)$. These properties are tabulated next.

We first consider the function $h(\alpha)$. Using the convolution theorem and other results for the Laplace transform together with the analytic behavior of the modified Bessel function $K_1(p)$, we can prove the following theorem.

Theorem 2. *Suppose that $f(t)$ is continuous and bounded on $t\geqslant 0$ and $f(0)=0$. Suppose that either* (ii) *or* (iii) *of Theorem* 1 *holds. Then $h(\alpha)$ is continuous bounded and positive on $\alpha\geqslant 0$, i.e. there exists a constant $M>0$ such that*

$$0\leqslant h(\alpha)\leqslant M,\quad \alpha\geqslant 0. \tag{3.6}$$

Also $h(0)=0$.

This theorem provides us with most of the information we need to know about $h(\alpha)$, but in order to carry out our shock analysis, we require a more detailed knowledge of its derivative $h'(\alpha)$ over the entire range $\alpha\geqslant 0$. It is therefore necessary to consider a restricted class of surface tractions $f(t)$. In particular, we shall focus attention on the breaking of a wave initiated at the boundary of the cavity by a continuous pulse of finite duration. To make this idea precise we make the following definition.

Definition. Let $f(t)\in C^{(\infty)}[0,t_*]$, suppose that $f(0)=0$ and

$$f(t)=0,\quad t\geqslant t_*.$$

Also suppose that $f'(t)>0$ on $0<t<t_0$ and $f'(t)<0$ on $t_0<t<t_*$, so that

$$0\leqslant f(t)\leqslant \sigma_0=f(t_0).$$

Then $f(t)$ is called a *pulse of duration time t_**. We note that $f(t)$ is continuous at $t=t_*$, but $f'(t)$ can have a finite jump at t_*.

A surface traction given by such a pulse models a shear stress on the wall of the cavity that rises continuously to a maximum σ_0 at $t = t_0$, then decreases to zero at $t = t_*$ and is zero thereafter. Eq. (2.14) is an example of a pulse of duration time t_* with $t_0 = t_*/2$. For such functions we can establish the following.

Theorem 3. *Suppose that $f(t)$ is a pulse of duration time t_* and suppose either* (ii) *or* (iii) *of Theorem* 1 *holds.*

(i) *$\phi(t)$ is also a pulse of duration time t_* with maximum $\epsilon_0 = \phi(t_0)$, where ϵ_0 is the smallest solution to* (2.37).

(ii) *In addition to the results of Theorem* 2, *$h(\alpha)$ also satisfies*

$$\lim_{\alpha\to\infty} h(\alpha) = 0$$

and

$$M = \max_{0\leqslant\alpha<\infty}\{h(\alpha)\} = h(\alpha'), \tag{3.7}$$

for some $\alpha' > 0$.

(iii) *$h'(\alpha)$ is bounded on $\alpha \geqslant 0$ and continuous on $\alpha \geqslant 0$ except possibly at $\alpha = t_*$, where it will have a finite jump if $f'(t)$ has a finite jump at $t = t_*$. Also*

$$h'(0) = 0, \quad \lim_{\alpha\to\infty} h'(\alpha) = 0$$

and $h'(\alpha)$ is increasing on $0 < \alpha < \alpha_f$ for some α_f, and $h'(\alpha) < 0$ for α sufficiently large.

Theorem 3 provides information about $h'(\alpha)$ for small and large values of α. In order to carry out subsequent analysis, we also need to know the behavior of $h'(\alpha)$ for intermediate values of α. Hence we plot $h'(\alpha)$ with (2.14) and for various choices of the parameters. This step reveals that $h'(\alpha)$ has the qualitative features shown in Fig. 1 for all choices of the parameters. In particular $h'(\alpha)$ has a bimodal shape on $0 < \alpha < \alpha_1$ and the peak time t_0 for $f(t)$ always lies in $\alpha_f < \alpha < \alpha_b$. In Fig. 1, the dotted line through t_* indicates the case in which $f'(t)$ is discontinuous at $t = t_*$. If $f'(t)$ is continuous, then $h'(\alpha)$ is continuous at

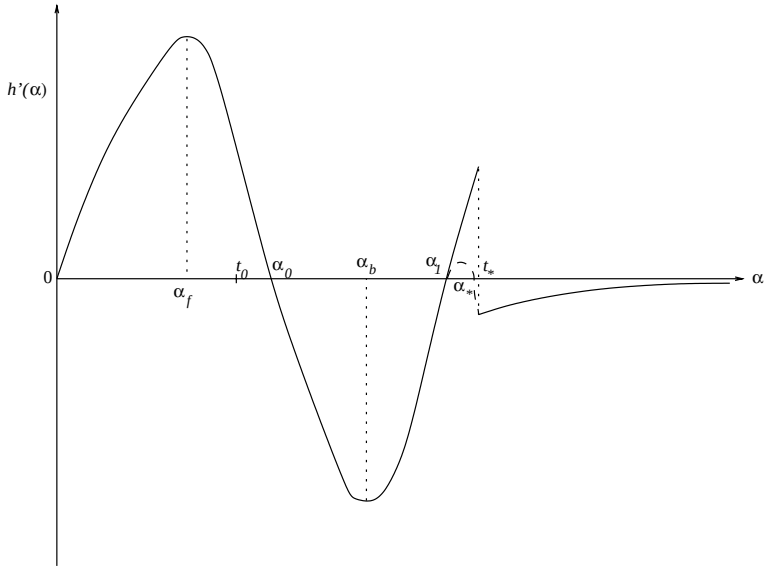

Fig. 1. Graph showing the behavior of $h'(\alpha)$ for a pulse of duration time t_*.

$\alpha = t_*$ and the curve in the neighbourhood of t_* is indicated by the hash marks. It is not tractable to prove in general that when $f(t)$ is a pulse, then $h'(\alpha)$ has the behavior shown in Fig. 1. Consequently, in the remaining part of this section it will be assume that if $f(t)$ is a pulse of duration time t_*, then the corresponding function $h'(\alpha)$ has the behavior shown in Fig. 1. This assumption does not appear to be a severe restriction, since for any pulse we tested numerically, the function $h'(\alpha)$ had this behavior. We always assume that either (ii) or (iii) of Theorem 1 holds to ensure that Eq. (2.36) defines $\phi(t)$ on $t \geqslant 0$. It now follows that if $f(t)$ is a pulse of duration time t_*, then $h(\alpha)$ has two local maxima, M_0 and M_*, on $\alpha \geqslant 0$ where

$$M_0 = h(\alpha_0)$$

and

$$M_* = h(t_*) \quad \text{or} \quad M_* = h(\alpha_*),$$

depending on whether $f'(t)$ is continuous or discontinuous at t_*. The maximum value of $h(\alpha)$ is then $M = \max\{M_0, M_*\}$.

We now obtain some results concerning the breaking of an axial shear wave that is initiated by a pulse of duration time t_* at the boundary of a cylindrical cavity. Since $f(0) = 0$, a wavefront leaves the boundary at $t = 0$ that is given by

$$t = r - 1.$$

A second wavefront leaves the boundary at $t = t_*$ and its equation is given by

$$t = t_* + r - 1 - \sum_{k=1}^{N} (2k+1)\gamma_k h^k(t_*) S_k(r). \tag{3.8}$$

The solution to our axial shear wave problem is zero ahead of the leading wavefront. Prior to shock initiation, the solution behind the leading wavefront is continuous with continuous derivatives except possibly along the back wavefront, where time and spatial derivatives of the solution will have a finite jump, if $f'(t)$ is discontinuous at t_*. For this case the front is an acceleration front.

Our shock analysis uses the fact that that the envelope constructed from (3.1) bounds regions of the rt-plane in which the solution (2.32) is multivalued. Such a region contains a shock path. Our results on shock development are valid under the assumptions made in obtaining the nonlinearized solution, i.e. $\|\boldsymbol{\gamma}\|$ is a small parameter and $\frac{\alpha}{r} \ll 1$. For a pulse of duration time t_* at the boundary, the relevant part of the solution is given by the characteristics for which $0 \leqslant \alpha \leqslant t_*$. So, in addition to the small parameter assumption, our results are valid if $t_* \ll 1$ or if breaking occurs for $r \gg t_*$. If neither of these conditions occur, then our results are valid if $\alpha \ll 1$, i.e. if a shock develops near the leading wavefront. The first result is an existence theorem for shock waves.

Theorem 4. *Let $f(t)$ be continuous on $t \geqslant 0$ and $f(0) = 0$, and such that Eq.* (2.36) *defines a unique $\phi(t)$ on $t \geqslant 0$. If there exists a subset of $\alpha > 0$ on which*

$$\gamma_1 h'(\alpha) > 0, \tag{3.9}$$

then an axial shear wave propagating from a cylindrical cavity into an unbounded medium that is initially at rest and unstressed, will always break.

Theorem 4 is proven in Appendix A. It is immediate from the behavior of $h'(\alpha)$, that a wave initiated at the boundary of a cylindrical cavity by a pulse of duration time t_*, will always break if $\gamma_1 \neq 0$.

Solutions to (3.1) will lead to an envelope of the family of characteristics that can be made up of several branches. A branch will bound a shock path. In order to describe each branch and the corresponding shock, we make the following definitions.

Definition. A branch of the envelope of characteristics is called a *primary branch* if the parametric equations (3.3), (3.4) have as domain either $0 < \alpha < \alpha_0$ or $\alpha_0 < \alpha < \alpha_1$. The associated shock will be called a *primary shock*.

Definition. A branch of the envelope of characteristics is called a *secondary branch* if the parametric equations (3.3), (3.4) have as domain either $\alpha_1 < \alpha < t_*$ or $t_* < \alpha < \infty$ when $f'(t)$ is discontinuous at t_*, and $\alpha_1 < \alpha < \alpha_*$ or $\alpha_* < \alpha < \infty$ when $f'(t)$ is continuous at t_*. The associated shock will be called a *back shock*.

Definition. If we replace the intervals in the above definitions by closed subintervals, then the corresponding branch of the envelope of characteristics will be called a *transient branch* and the associated shock a *transient shock*.

As we will see later, (r,t) are unbounded on a primary or secondary branch and are bounded on a transient branch. So a primary or back shock propagates indefinitely, but a transient shock propagates only for a finite length of time. Also, an equivalent definition of a transient branch would be one on which (r,t) are bounded.

We now present some theorems which describe the possible shock paths that can occur after a continuous axial shear wave breaks.

Theorem 5. *Let $f(t)$ be a pulse of duration time t_*. Suppose $\gamma_1 \neq 0$ and let $P_N(x)$ be the polynomial of degree N*

$$P_N(x) = \sum_{k=1}^{N} (2k+1)\gamma_k x^k. \tag{3.10}$$

(i) *If*

$$\max_{0 \leqslant x \leqslant M_0} \{P_N(x)\} < 1, \tag{3.11}$$

then a primary shock develops near the front (or back) of the wave if $\gamma_1 > 0$ (or $\gamma_1 < 0$) and breaking occurs at a cusp on the primary branch of the envelope.

(ii) *If*

$$\max_{0 \leqslant x \leqslant M_*} \{P_N(x)\} < 1, \tag{3.12}$$

then a back shock develops near or on the back acceleration front.

(iii) *If $P'_N(x) \neq 0$ on $0 < x < M$, then no other shocks occur.*

Theorem 5 is proven in Appendix B. It shows that if $\gamma_1 \neq 0$, a primary shock and a back shock will always occur, and these are the only shocks that propagate indefinitely. As well, if $P'_N(x) \neq 0$ on $0 < x < M$, then there are no other shocks. If $P'_N(x)$ is zero at least once on $0 < x < M$, then a transient shock could also occur for axial shear wave propagation. We shall describe in detail the situation when $P'_N(x)$ has a single zero. The analysis when there are several zeros would be handled in a similar way.

If x_1 is the only zero of $P'_N(x)$, where $0 < x_1 < M$, then two transient shocks could possibly develop. If $0 < x_1 < M_0$, then a transient shock could occur, where the domain of (3.3), (3.4) would be a subset of $0 < \alpha < \alpha_1$. For this case, we will use the terminology *primary transient shock*. If $0 < x_1 < M_*$, then a

transient shock could occur near the back acceleration front. Our theorems on transient shocks are stated without proof. As in Theorem 5, the proofs involve examining Eq. (3.1). The next theorem gives condition under which a single primary transient shock occurs.

Theorem 6. *Let $f(t)$ be a pulse of duration time t_*. Suppose $\gamma_1 \neq 0$,* (3.11) *holds and $P_N'(x)$ has a single zero, x_1, on $0 < x < M_0$, where x_1 is a simple zero. Define*

$$r_1(\alpha) = \frac{h(\alpha)}{x_1},$$

$$Q_1(\alpha) = h'(\alpha) L(r_1(\alpha), \alpha)$$

and let $\alpha_1^{(1)} < \alpha < \alpha_1^{(2)}$ be the subinterval of $0 < \alpha < \alpha_1$ on which $r_1(\alpha) > 1$. Let

$$Q(\gamma_1) = \begin{cases} \max\limits_{\alpha_0 \leqslant \alpha \leqslant \alpha_1^{(2)}} \{Q_1(\alpha)\}, & \text{if } \gamma_1 > 0, \\ \max\limits_{\alpha_1^{(1)} \leqslant \alpha \leqslant \alpha_0} \{Q_1(\alpha)\}, & \text{if } \gamma_1 < 0. \end{cases} \tag{3.13}$$

(i) *If $Q(\gamma_1) > 1$, then the envelope of characteristics has a closed bounded branch (a primary transient branch). The branch has two cusps at which (r, t) obtain their minimum values $(r_{\mathrm{B}}^{(\mathrm{tr})}, t_{\mathrm{B}}^{(\mathrm{tr})})$ at one of the cusps, and their maximum values $(r_{\mathrm{T}}^{(\mathrm{tr})}, t_{\mathrm{T}}^{(\mathrm{tr})})$ at the other. The quantities $r_{\mathrm{B}}^{(\mathrm{tr})}$ and $t_{\mathrm{B}}^{(\mathrm{tr})}$ are the breaking distance and time of the transient shock. The quantities $r_{\mathrm{T}}^{(\mathrm{tr})}$ and $t_{\mathrm{T}}^{(\mathrm{tr})}$ are the distance and time at which the transient shock terminates. The primary transient shock breaks and terminates at the front (or back) of the wave if $\gamma_1 < 0$ (or $\gamma_1 > 0$).*

(ii) *If $Q(\gamma_1) \leqslant 1$, then a primary transient shock does not occur.*

If $0 < x_1 < M_*$, then a transient shock could occur near the back acceleration front, and we could establish a similar result with M_0 replace by M_*.

If all the material parameters γ_k are nonnegative, then $P_N'(x) \neq 0$ on $0 \leqslant x \leqslant M$ and a transient shock never occurs. For several materials considered by Alexander (1968), Tschoegl (1971), James et al. (1975) and Haines and Wilson (1979), $N = 2$ and $\gamma_1 \gamma_2 < 0$. In the remaining part of this section, we list results for this interesting situation. For completeness, we first summarize the restrictions on the material parameters imposed by Theorem 1.

Theorem 7. *Let $f(t)$ be a pulse of duration time t_*.*

(i) *If $\gamma_k \geqslant 0$ for all k, then $\phi(t)$ exists and is a pulse of duration time t_*.*

(ii) *If $N = 2$, $\gamma_1 < 0$, $\gamma_2 > 0$ and*

$$\gamma_2 \geqslant \frac{9}{10}\gamma_1^2,$$

then $\phi(t)$ exists and is a pulse of duration time t_*.

(iii) *If $N = 2$, $\gamma_1 < 0$, $\gamma_2 > 0$ and*

$$\gamma_2 < \frac{9}{10}\gamma_1^2, \tag{3.14}$$

$$\sigma_0 \leqslant \frac{4}{5} \frac{\sqrt{\gamma} - 2\gamma_1}{(\sqrt{\gamma} - 3\gamma_1)^{3/2}}, \tag{3.15}$$

where

$$\gamma = 9\gamma_1^2 - 10\gamma_2, \tag{3.16}$$

then $\phi(t)$ *exists and is a pulse of duration time* t_*.

(iv) *If* $N = 2$, $\gamma_1 > 0$, $\gamma_2 < 0$ *and* (3.15) *holds then* $\phi(t)$ *exists and is a pulse of duration time* t_*.

Theorem 8. *Let* $f(t)$ *be a pulse of duration time* t_* *and suppose that* $N = 2$, $\gamma_1\gamma_2 < 0$ *and one of* (ii)–(iv) *of Theorem* 7 *holds.*

(i) *If*

$$-\frac{\gamma_1}{\gamma_2} \geqslant \frac{10}{3}M_0, \tag{3.17}$$

then a primary transient shock will not occur.

(ii) *If*

$$-\frac{\gamma_1}{\gamma_2} < \frac{10}{3}M_0 \tag{3.18}$$

and $Q(\gamma_1) \leqslant 1$, *where* $Q(\gamma_1)$ *is given by* (3.13) *and*

$$Q_1(\alpha) = h'(\alpha)\{3\gamma_1[1 + \ln r_1(\alpha)] + 10\gamma_2 h(\alpha)\}, \quad r_1(\alpha) = -\frac{10\gamma_2}{3\gamma_1}h(\alpha),$$

then a primary transient shock will not occur.

Theorem 9. *Let* $f(t)$ *be a pulse of duration time* t_* *and suppose that* $N = 2$, $\gamma_1\gamma_2 < 0$ *and one of* (ii)–(iv) *of Theorem* 7 *holds. If*

$$-\frac{\gamma_1}{\gamma_2} < \frac{10}{3}M_0 \tag{3.19}$$

and $Q(\gamma_1) > 1$, *and one of the following holds.*

(i) $\gamma_1 > 0$, $\gamma_2 < 0$ *and*

$$-\frac{9\gamma_1^2}{20\gamma_2} < 1, \tag{3.20}$$

(ii) $\gamma_1 < 0$, $\gamma_2 > 0$ *and*

$$\frac{5M_0}{3} < -\frac{\gamma_1}{\gamma_2}, \tag{3.21}$$

(iii) $\gamma_1 < 0$, $\gamma_2 > 0$ *and*

$$-\frac{\gamma_1}{\gamma_2} < \frac{5M_0}{3}, \tag{3.22}$$

$$M_0(3\gamma_1 + 5\gamma_2 M_0) < 1. \tag{3.23}$$

Then a primary transient shock occurs, and the shock breaks and terminates at a cusp on the primary transient branch.

A similar result can be established concerning a transient shock near the back acceleration front. As well if $N \geqslant 3$, then $P_N'(x)$ could have more than one zero. We could then have several primary and back transient

shocks occurring. The above theorems indicate how the analysis would proceed for this situation. Finally, we note that if $\gamma_1 = 0$, only transient shocks can develop.

4. Numerical results

In this section, we illustrate our theorems on shock development of axial shear waves. The theorems are used to predict what shocks will occur and to estimate the breaking time of each one. The envelope of characteristics can be found by solving (3.1) and a region bounded by a branch of the envelope approximates the location of the corresponding shock path. In order to use the theorems efficiently, it is necessary to readily evaluate $h(\alpha)$ and $h'(\alpha)$.

The function $h(\alpha)$ is defined in terms of $G(\alpha)$ by (2.34) and since $G(\alpha)$ is given by (2.31), we can evaluate it by numerically inverting a Laplace transform. In order to carry out the numerical inversion, we need an analytic expression for $\bar{\phi}(p) = \mathscr{L}\{\phi(t)\}$. So we need an appropriate approximation to $\phi(t)$ in terms of the given boundary value $f(t)$. From (2.36), a first order approximation is

$$\phi(t) = f(t) - 2\sum_{k=1}^{N} \gamma_k f^{2k+1}(t) + \mathrm{O}\left(\|\gamma\|^2\right),$$

which is uniform in t when $f(t)$ is a pulse of duration time t_*. This approximation is consistent with the approximation made in constructing the nonlinearized solution, but is not particularly useful when $\sigma_0 > 1$. Since $\phi(t)$ is a pulse of duration time t_* when $f(t)$ is a pulse of duration time t_*, a useful approximation is

$$\phi(t) = \frac{\epsilon_0}{\sigma_0} f(t),$$

where ϵ_0 is found from (2.37). This simple approximation preserves the appropriate character of the boundary value and will be used to find $\bar{\phi}(p)$ when $\sigma_0 > 1$.

To test the usefulness and validity of the theorems of the previous section, we solve the system (2.19) and (2.21) numerically. We use the relaxation scheme for conservation laws developed by Jin and Xin (1995). This method has advantages over other high-order accurate schemes. It uses neither Riemann solvers spatially nor nonlinear equation solvers temporally. The method has excellent shock capturing abilities and shows no numerical dispersion at the shock. When implementing the relaxation scheme, the value of $\phi(t)$ is found by solving the nonlinear equation (2.36) numerically.

All results are for the boundary value (2.14). Since $f'(t)$ has a finite jump at $t = 0, t_*$, the leading and back wavefronts are acceleration fronts. Results in Fig. 2 are for $\sigma_0 = 2$, $t_* = 1$ and $N = 1$, $\gamma_1 = 0.1$. Using Theorem 5, we find that a primary shock breaks near the front of the pulse at $(r_{\mathrm{B}}^{(\mathrm{p})}, t_{\mathrm{B}}^{(\mathrm{p})}) = (1.84, 0.92)$, a back shock breaks at $(r_{\mathrm{B}}^{(\mathrm{b})}, t_{\mathrm{B}}^{(\mathrm{b})}) = (4.72, 4.69)$ and no other shocks occur. Fig. 3 shows the shock pattern, or more precisely, the primary and secondary branch of the envelope together with the acceleration fronts. The back acceleration front is found using (3.8). The numerical solution shown in Fig. 2 exhibits the behavior predicted by our shock theorems. The estimate of breaking times are reasonably accurate. A primary shock is clearly visible at the front of the pulse for $t \geqslant 2$ and a small back shock can be seen for $t \geqslant 5$.

The remaining numerical results are for a material with $N = 2$ and $\gamma_1 = -0.029$, $\gamma_2 = 0.0027$. These values are found from the set of C_{ij} for the second rubber-like material considered by Haines and Wilson (1979). We consider first a pulse of duration time $t_* = 1$ and maximum $\sigma_0 = 2$. Theorem 5 indicates that a primary shock breaks near the back of the pulse at $(r_{\mathrm{B}}^{(\mathrm{p})}, t_{\mathrm{B}}^{(\mathrm{p})}) = (3.06, 2.94)$ and a back shock does not occur in finite time. Our theorems also indicate that no transient shocks occur. The shock pattern is shown in Fig. 4 and the numerical solution in Fig. 5. The primary shock is clearly visible at the back of

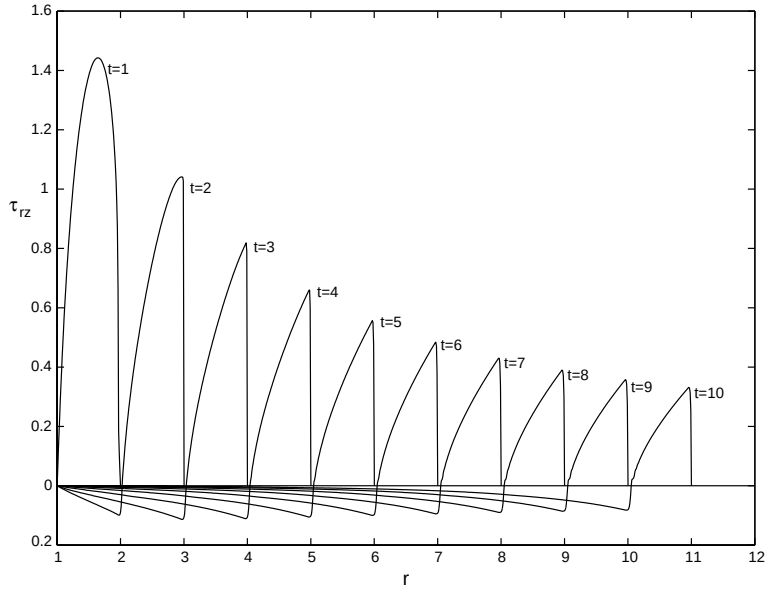

Fig. 2. Variation of τ_{rz} with nondimensional r for $N = 1$, $\gamma_1 = 0.1$ and boundary value (2.14) with $\sigma_0 = 2$, $t_* = 1$.

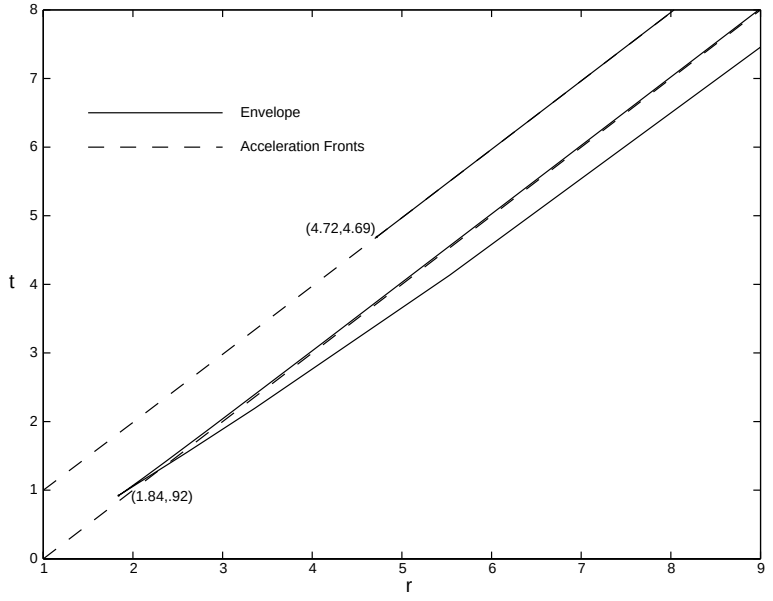

Fig. 3. Branches of the envelope for $N = 1$, $\gamma_1 = 0.1$ and boundary value (2.14) with $\sigma_0 = 2$, $t_* = 1$.

the pulse for $t \geqslant 3$. Finally, we consider a pulse with $\sigma_0 = 4$ and $t_* = 1$. Theorem 9 reveals that a primary transient shock breaks at $(r_{\mathrm{B}}^{(\mathrm{t_r})}, t_{\mathrm{B}}^{(\mathrm{t_r})}) = (1.47, 0.79)$ and terminates at $(r_{\mathrm{T}}^{(\mathrm{t_r})}, t_{\mathrm{T}}^{(\mathrm{t_r})}) = (6.08, 5.94)$. There is no back transient shock. Also by Theorem 5, we find that the primary shock breaks near the back of the

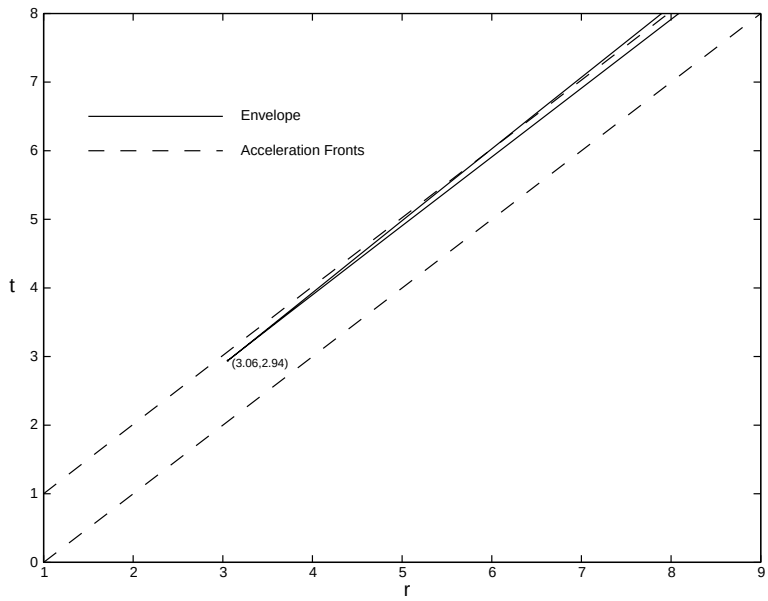

Fig. 4. Primary branch of the envelope for $N = 2$, $\gamma_1 = -0.029$, $\gamma_2 = 0.0027$ and boundary value (2.14) with $\sigma_0 = 2$, $t_* = 1$.

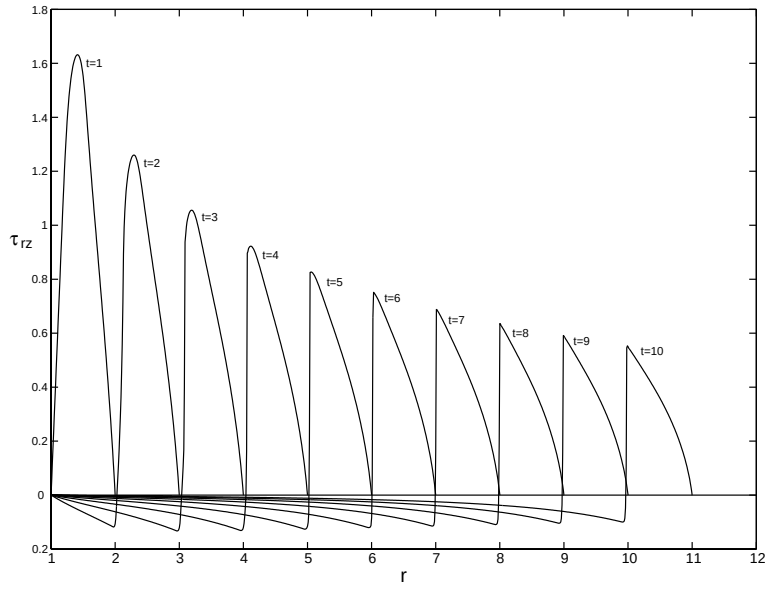

Fig. 5. Variation of τ_{rz} with nondimensional r for $N = 2$, $\gamma_1 = -0.029$, $\gamma_2 = 0.0027$ and boundary value (2.14) with $\sigma_0 = 2$, $t_* = 1$.

pulse at $(r_B^{(p)}, t_B^{(p)}) = (2.04, 1.94)$, and that a back shock does not break in finite time. The numerical solution in Fig. 6 shows the pulse as it leaves the boundary. The figure shows the development of the transient shock near the front of the pulse and the primary shock at the back. Fig. 7 shows the numerical

solution until after the transient shock terminates. The shock pattern obtained from our shock theorems is shown in Fig. 8.

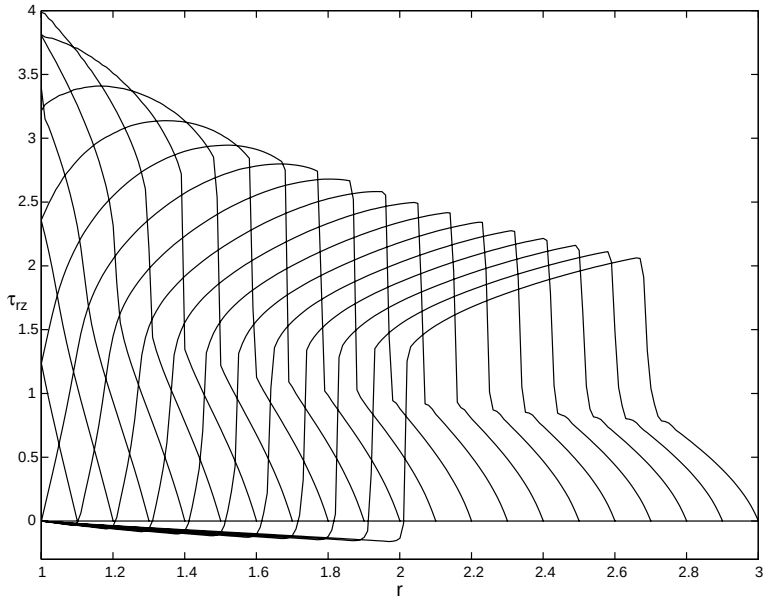

Fig. 6. Variation of τ_{rz} with nondimensional r at $t = 0.1, 0.2, \ldots, 2$ for $N = 2$, $\gamma_1 = -0.029$, $\gamma_2 = 0.0027$ and boundary value (2.14) with $\sigma_0 = 4$, $t_* = 1$.

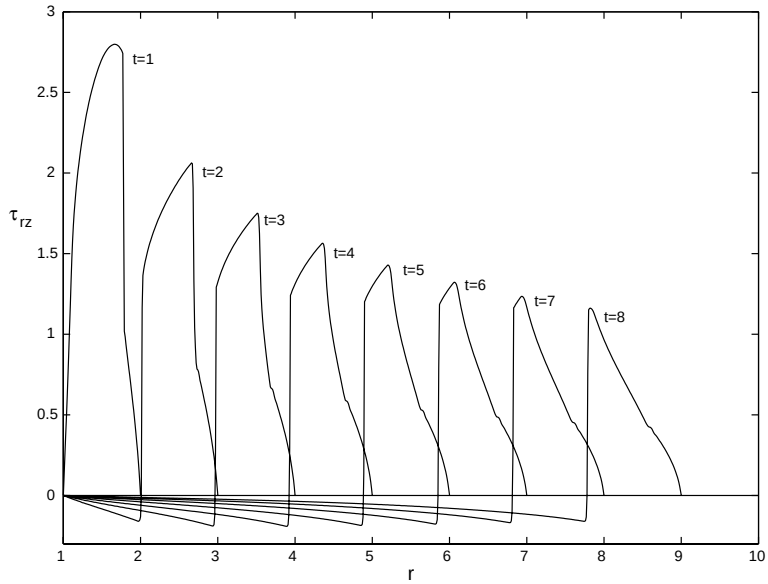

Fig. 7. Variation of τ_{rz} with nondimensional r for $N = 2$, $\gamma_1 = -0.029$, $\gamma_2 = 0.0027$ and boundary value (2.14) with $\sigma_0 = 4$, $t_* = 1$.

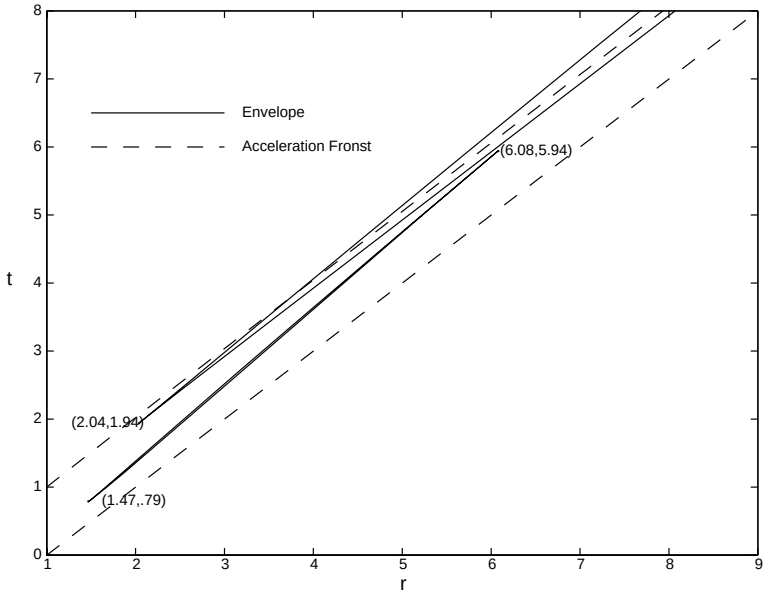

Fig. 8. Primary and transient branch of the envelope for $N = 2$, $\gamma_1 = -0.029$, $\gamma_2 = 0.0027$ and boundary value (2.14) with $\sigma_0 = 4$, $t_* = 1$.

5. Conclusions

The theorems presented in Section 3 provide a complete picture of the shock pattern for axial shear wave propagation after a continuous pulse breaks. A primary and back shock always occur if and only if $\gamma_1 \neq 0$. The primary shock breaks at the front (or back) of the pulse if $\gamma_1 > 0$ (or $\gamma_1 < 0$). Since

$$\max_{t_* \leqslant \alpha < \infty} |h'(\alpha)| \ll \max_{\alpha_0 \leqslant \alpha \leqslant \alpha_1} |h'(\alpha)|,$$

in all our numerical work, a back shock was not observed if $\gamma_1 < 0$.

The polynomial $P_N(x)$, whose coefficients involve the material parameters, plays a significant role in our analysis. If $P'_N(x) \neq 0$ on $0 < x < M$, then only a primary and a back shock will develop. If $P'_N(x) = 0$ on $0 < x < M$, then a transient shock can occur. The phenomenon of a transient shock has not been reported in other studies on nonlinear axially symmetric shear wave propagation. Conditions concerning the existence of a transient shock were given when $P'_N(x)$ vanishes only once on $0 < x < M$. If $N = 2$ then $P'_N(x)$ has only one zero. So this case is of particular interest, since most experimental results found in the literature for materials modelled by a strain energy function (1.3) use $N = 2$.

A knowledge of certain analytical properties of $h(\alpha)$ and its derivative $h'(\alpha)$ is necessary in order to determine the shock pattern for axial shear waves. The function $h(\alpha)$ is defined by (2.34) and is related to the boundary value through the inverse transform (2.31). Our shock pattern theorems are valid for a wave generated by a pulse $f(t)$ of finite duration time, provided we assume that $h'(\alpha)$ has the behavior shown in Fig. 1. This assumption appears to be reasonable since, for any particular pulse $f(t)$ that we considered, the corresponding function $h'(\alpha)$ had this behavior.

The shock pattern determined in this paper is for axial shear wave propagation. Similar results can be obtained for torsional shear waves propagating alone. For combined axial and torsional shear wave propagation, the situation is more complicated. This case needs further examination.

Finally, as the numerical solutions indicate, our shock theorems provide a direct and accurate way of estimating the breaking distance and time of a shock. As well, the region bounded by a branch of the envelope of characteristics contains a shock path, giving an approximate location of the shock path.

Appendix A. Proof of Theorem 4

From the definition (3.1) of $L(r,\alpha)$, we have

$$L(1,\alpha)=0,$$

and for fixed α

$$L(r,\alpha)=3\gamma_1\ln r\left[1+\mathrm{O}\left(\frac{1}{\ln r}\right)\right],\quad \text{as } r\to\infty,$$

$$\frac{\partial L(r,\alpha)}{\partial\alpha}=\frac{3\gamma_1}{r}\left[1+\mathrm{O}\left(\frac{1}{r}\right)\right],\quad \text{as } r\to\infty.$$

As well, $L(r,\alpha)$ is a continuous function of (r,α) for $r\geqslant 1$, $\alpha\geqslant 0$. So if (3.9) holds, then Eq. (3.1) always has a solution in $r>1$. Hence an envelope always exists and a wave will break, at least for r sufficiently large.

Appendix B. Proof of Theorem 5

(i) Observe that $L(r,\alpha)$ is a continuous function of (r,α) on $r\geqslant 1$, $\alpha\geqslant 0$ and such that $L(1,\alpha)=0$ and for fixed α, $L(r,\alpha)\to\infty$ as $r\to\infty$.

Now consider first the case in which $P_N'(x)\neq 0$ on $0<x<M$ and note from (3.2) that

$$\frac{\partial L}{\partial r}=\frac{1}{r}P_N'\left(\frac{h(\alpha)}{r}\right).$$

Since $0\leqslant h(\alpha)\leqslant M$ and $r\geqslant 1$, then $0\leqslant\frac{h(\alpha)}{r}\leqslant M$. So for fixed $\alpha\geqslant 0$, $L(r,\alpha)$ is an increasing (or decreasing) function of r on $r>1$ when $\gamma_1>0$ (or $\gamma_1<0$). It follows that Eq. (3.1) has a unique solution (3.3) on $0<\alpha<\alpha_0$ (or $\alpha_0<\alpha<\alpha_1$) if $\gamma_1>0$ (or $\gamma_1<0$). Hence we have a primary branch. The solution $E(\alpha)$ and its derivative $E'(\alpha)$ are continuous and

$$\lim_{\alpha\to 0+}E(\alpha)=\infty,\quad \lim_{\alpha\to\alpha_0-}E(\alpha)=\infty,\quad \gamma_1>0,$$

$$\lim_{\alpha\to\alpha_0+}E(\alpha)=\infty,\quad \lim_{\alpha\to\alpha_1-}E(\alpha)=\infty,\quad \gamma_1<0.$$

If $N=1$ and $\gamma_1>0$ (or $\gamma_1<0$), then $E(\alpha)$ decreases steadily to a minimum at α_f (or α_b) then increases steadily. If $N\geqslant 2$, this behavior is not strictly true, but since

$$E'(\alpha)\frac{\partial L}{\partial r}=-\frac{h''(\alpha)}{h'^2(\alpha)}+\mathrm{O}(\|\boldsymbol{\gamma}\|),$$

it will be true within our small parameter assumption, but now $E(\alpha)$ will attain its minimum in a neighbourhood of α_f (or α_b) if $\gamma_1>0$ (or $\gamma_1<0$).

Now a straight-forward calculation using (2.33) and (3.1) reveals that

$$T'(\alpha)=E'(\alpha)\left[1-P_N\left(\frac{h(\alpha)}{E(\alpha)}\right)\right]. \tag{B.1}$$

So (3.11) implies that $T'(\alpha)$ and $E'(\alpha)$ have the same sign on $0 < \alpha < \alpha_1$. Hence (r, t) decrease steadily from infinity on the primary branch to a cusp $(r_B^{(p)}, t_B^{(p)})$, where r and t obtain their minimum values, and then increase steadily back to infinity. The quantities $r_B^{(p)}$ and $t_B^{(p)}$ are the breaking distance and time of the primary shock. Since $\alpha_f < t_0 < \alpha_b$, the characteristics labelled $\alpha = \alpha_f$ and $\alpha = \alpha_b$ leave the boundary $r = 1$ before and after t_0 respectively. So the primary shock breaks at the front (or back) of the wave if $\gamma_1 > 0$ (or $\gamma_1 < 0$).

If $P_N'(x) = 0$ on $0 < x < M$, then L is not necessarily monotonic on $r > 1$, but there will exist $r_0(\alpha) > 1$ such that for fixed $\alpha \geqslant 0$, $L(r, \alpha)$ is monotonic for $r > r_0(\alpha)$. It then follows that Eq. (3.1) has a unique continuous solution (3.3) on the entire interval $0 < \alpha < \alpha_0$ (or $\alpha_0 < \alpha < \alpha_1$) if $\gamma_1 > 0$ (or $\gamma_1 < 0$). So we again get a primary branch with all the properties given above. For this case, other solutions can also exist but each would define a continuous function $E(\alpha)$ on a closed subinterval of $0 < \alpha < \alpha_0$ or $\alpha_0 < \alpha < \alpha_1$. The corresponding parametric equations would then give a transient branch.

(ii) Since the behavior of $h'(\alpha)$ on $\alpha_1 < \alpha < \infty$ is similar to the behavior on $0 < \alpha < \alpha_1$, the arguments used in (i) can be applied to show the existence of a secondary branch. Its structure is the same as the primary branch, when $f'(t)$ is continuous at t_*, and breaking occurs at a cusp, $(r_B^{(b)}, t_B^{(b)})$, on the envelope near the back acceleration front. If $f'(t)$ is not continuous at t_*, the secondary branch has a different structure. For this case, when $\gamma_1 > 0$, the secondary branch comes in from infinity and terminates at the back acceleration front. If $\gamma_1 < 0$, the secondary branch goes out from the back acceleration front to infinity. In either case, when $f'(t)$ is discontinuous at t_*, the back shock path is bounded by the envelope and the back acceleration front, and breaking occurs at the back acceleration front.

(iii) As shown in (i) and (ii) above, when $P_N'(x) \neq 0$ on $0 < x < M$, we only obtain a primary and a secondary branch of the envelope of characteristics. So, for this case, only a primary and a back shock will occur.

References

Alexander, H., 1968. A constitutive relation for rubber-like materials. Int. J. Eng. Sci. 6, 549–563.

Barclay, D.W., 1999. Shock front analysis for axial shear wave propagation in a hyperelastic compressible solid. Acta Mech. 133 (1–4), 105–129.

Barclay, D.W., 2004. Shock calculations for axially symmetric shear wave propagation in a hyperelastic incompressible solid. Int. J. Non-Linear Mech. 39 (1), 101–121.

Fu, Y., Scott, N., 1991. Transverse cylindrical simple waves in elastic non-conductors. Int. J. Solids Struct. 27, 547–563.

Haddow, J., Lorimer, S., Tait, R., 1987a. Non-linear combined axial and torsional shear wave propagation in an incompressible hyperelastic solid. Int. J. Non-Linear Mech. 22 (4), 297–306.

Haddow, J., Lorimer, S., Tait, R., 1987b. Nonlinear axial shear wave propagation in a hyperelastic incompressible solid. Acta Mech. 66, 205–216.

Haines, D., Wilson, W., 1979. Strain energy density function for rubber-like materials. J. Mech. Phys. Solids 27, 345–360.

James, A., Green, A., Simpson, G., 1975. Strain energy functions of rubber. I. characterization of gum vulcanizates. J. Appl. Polym. 19, 2033–2058.

Jin, S., Xin, Z., 1995. The relaxation schemes for systems of conservation laws in arbitrary space dimensions. Commun. Pure Appl. Math. 48, 235–276.

Ogden, R., 1984. Non-Linear Elastic Deformations. Ellis Horwood, Chichester.

Tait, R., Lorimer, S., Haddow, J., 1989. Finite amplitude elastic wave propagation. Wave Motion 11, 251–260.

Tschoegl, N.W., 1971. Constitutive equations for elastometers. J. Polym. Sci. A 19, 1959–1970.

Whitham, G., 1974. Linear and Nonlinear Waves. John Wiley & Sons, New York.